Properties of Pseudoscalar Flavour-Singlet Mesons from $N_f = 2+1+1$ Twisted Mass Lattice QCD

Krzysztof Cichy

NIC, DESY, Platanenallee 6, D-15738 Zeuthen, Germany
& Adam Mickiewicz University, Faculty of Physics, Umultowska 85, 61-614 Poznan, Poland
krzysztof.cichy@desy.de

Vincent Drach, Karl Jansen

NIC, DESY, Platanenallee 6, D-15738 Zeuthen, Germany
vincent.drach,karl.jansen@desy.de

Elena Garcia-Ramos

NIC, DESY, Platanenallee 6, D-15738 Zeuthen, Germany
& Humboldt Universität zu Berlin, Newtonstrasse 15, D-12489 Berlin, Germany
elena.garcia.ramos@desy.de

Chris Michael

Theoretical Physics Division, Department of Mathematical Sciences,
The University of Liverpool, Liverpool L69 3BX, UK
C.Michael@liverpool.ac.uk

Konstantin Ottnad[*]**, Carsten Urbach, Falk Zimmermann**[†]

Institut für Strahlen- und Kernphysik, Rheinische Friedrich-Wilhelms-Universität Bonn
Nussallee 14-16, 53115 Bonn
ottnad,urbach,fzimmermann@hiskp.uni-bonn.de

For the ETM Collaboration

We study properties of pseudoscalar flavour-singlet mesons from Wilson twisted mass lattice QCD with $N_f = 2+1+1$ dynamical quark flavors. Results for masses are presented at three values of the lattice spacing and light quark masses corresponding to values of the pion mass from 230 MeV to 500 MeV. We briefly discuss scaling effects and the light and strange quark mass dependence of M_η. In addition we present an exploratory study using Osterwalder-Seiler type strange and charm valence quarks. This approach avoids some of the complications of the twisted mass heavy doublet. We present first results for matching valence and unitary actions and a comparison of statistical uncertainties.

The 30 International Symposium on Lattice Field Theory - Lattice 2012,
June 24-29, 2012
Cairns, Australia

---

[*]Speaker.

[†]Speaker.

1. Introduction

A remarkable feature of the η' meson in comparison to the pions, the kaons and the η meson is its extraordinary high mass of about 1 GeV: while pions consist only of light quarks and - therefore - exhibit a rather small mass around 140 MeV, strange quark contributions rise the mass of the four kaons and the η meson to 500 - 600 MeV. However, the larger strange quark mass cannot explain the mass value of the η' meson. On the QCD level, the reason for the mass gap is thought to be the breaking of the $U_A(1)$ symmetry by quantum effects.

Although lattice QCD provides access to flavour singlet pseudo-scalar states, significant contributions from quark disconnected diagrams complicate the determination of their properties. This might be the reason for the rather short list of publications covering these mesons. Recent studies for $2+1$ dynamical quark flavours can be found in [1, 2, 3] and [4]. For a recent publication with $N_f = 2$ Wilson twisted mass fermions see Ref. [5].

In this proceeding contribution, we build on a recent paper of some of the authors [6] and discuss the determination of η and η' meson masses and the mixing angle using the Wilson twisted mass lattice QCD formulation [7] with $N_f = 2 + 1 + 1$ dynamical quark flavours. Compared to Ref. [6] we present results for an additional ensemble, which allows us to better control systematic uncertainties. The final results stay virtually unaffected compared to Ref. [6].

The results presented in Ref. [6] were extracted for the unitary case, with identical sea and valence quark regularisations. In addition we discuss a mixed action approach with so called Osterwalder-Seiler strange and charm valence quarks [8]. Possible advantages of such an approach are a powerful variance reduction technique for strange and charm quarks [5, 9] and reduced twisted mass induced isospin splitting in the strange/charm doublet. We discuss how to perform the matching of valence and sea formulation and present first results for the variance reduction.

2. Lattice actions

The results we present are based on gauge configurations provided by the European Twisted Mass Collaboration (ETMC) and correspond to three values of the lattice spacing, $a = 0.061$ fm, $a = 0.078$ fm and $a = 0.086$ fm. The pion masses range from 230 to 500 MeV [10, 11]. A list of the investigated ensembles is given in Table 1. For setting the scale we use throughout this proceeding contribution the Sommer parameter $r_0 = 0.45(2)$ fm [11].

The Dirac operators for u and d quarks [7] reads

$$D_\ell = D_W + m_0 + i\mu_\ell \gamma_5 \tau^3 \tag{2.1}$$

with μ_ℓ the bare light twisted mass parameter. For the heavy doublet of c and s quarks [12] the Dirac operator reads

$$D_h = D_W + m_0 + i\mu_\sigma \gamma_5 \tau^1 + \mu_\delta \tau^3 . \tag{2.2}$$

D_W denotes the standard Wilson operator and the τ^i are Pauli matrices acting in flavour space. The value of the bare quark mass m_0 was tuned to its critical value [13, 10], leading to automatic order $\mathscr{O}(a)$ improvement at maximal twist [14], which represents the most notable advantage of

tmLQCD. The two bare quark masses μ_σ, μ_δ are related to the physical charm and strange quark mass via

$$m_{c,s} = \mu_\sigma \pm Z\,\mu_\delta\,, \tag{2.3}$$

where $Z = Z_P/Z_S$ defines the ratio of pseudo-scalar and scalar renormalisation constants Z_P and Z_S. We denote quark doublets in the physical basis by $\psi_{\ell,h}$ and in the twisted basis by $\chi_{\ell,h}$. In the continuum they are related by exact axial rotations

$$\psi_{\ell,h} = e^{i\pi\gamma_5\tau^{3,1}/4}\,\chi_{\ell,h}\,, \quad \bar\psi_{\ell,h} = \bar\chi_{\ell,h}\,e^{i\pi\gamma_5\tau^{3,1}/4}\,. \tag{2.4}$$

The main drawback of this formulation is the breaking of flavour symmetry at finite values of the lattice spacing, which was shown to affect mainly the value of the neutral pion mass [15, 16, 17]. Furthermore, for the non-degenerate quark doublet this introduces mixing between charm and strange quarks.

This complication can be circumvented in a mixed action approach using so-called Osterwalder-Seiler (OS) type quarks in the valence sector for strange and charm quarks [8]. Formally, we introduce one twisted doublet each for valence strange and valence charm quarks [8, 18]. Therefore, in the valence strange and charm sector flavour mixing is avoided. It was shown in Ref. [8] that automatic $\mathscr{O}(a)$ improvement is not spoiled by this approach and that unitarity is restored in the continuum limit.

Formally, we have introduced two strange (charm) quarks differing in the sign of the twisted mass. We will denote the one with positive sign with s (c) and the other one with s' (c'). With μ_s and μ_c we denote the bare OS strange and charm twisted masses, respectively.

The two actions in the sea and the valence sector must be matched appropriately. This matching can be performed using different observables: firstly, one can match using the quark mass values

$$\mu_{s,c} = \mu_\sigma \pm Z\,\mu_\delta\,,$$

requiring the knowledge of the ratio of renormalisation constants Z; secondly, unitary and OS kaon mass values can be matched. For the OS kaons we have the possibility to define the following OS interpolating fields in the twisted basis

$$\mathscr{O}_{K^{\text{os}}} \equiv \bar\chi_{s'}\chi_d(x)\,, \qquad \mathscr{O}_{K^+} \equiv \bar\chi_s\,i\gamma_5\chi_d\,,$$

which will lead to different kaon mass values at finite values of the lattice spacing. The corresponding kaon masses will be denoted by $M_{K^{\text{os}}}$ and M_{K^+}, respectively. The unitary kaon mass value is denoted by M_K. Note that there is no isospin splitting for the kaons in $N_f = 2+1+1$ Wilson twisted mass lattice QCD [19].

Thirdly, one can use the mass of the artificial η_s meson – a pion made out of strange quarks – to match sea and valence actions. M_{η_s} can be determined from the connected only correlation function of the following operator

$$\mathscr{O}_{\eta_s} \equiv \frac{1}{\sqrt{2}}(\bar\chi_s\,\chi_s - \bar\chi_{s'}\,\chi_{s'})\,.$$

Similarly, one can define matching observables for the charm quark. However, as we are mainly interested in η and η' mesons, we expect little impact from the charm quark. Therefore, we

ensemble	β	$a\mu_\ell$	$a\mu_\sigma$	$a\mu_\delta$	L/a	N_{conf}	N_s	N_b
A30.32	1.90	0.0030	0.150	0.190	32	1367	24	5
A40.24	1.90	0.0040	0.150	0.190	24	2630	32	10
A40.32	1.90	0.0040	0.150	0.190	32	863	24	4
A60.24	1.90	0.0060	0.150	0.190	24	1251	32	5
A80.24	1.90	0.0080	0.150	0.190	24	2449	32	10
A100.24	1.90	0.0100	0.150	0.190	24	2493	32	10
A80.24s	1.90	0.0080	0.150	0.197	24	2517	32	10
A100.24s	1.90	0.0100	0.150	0.197	24	2312	32	10
B25.32	1.95	0.0025	0.135	0.170	32	1484	24	5
B35.32	1.95	0.0035	0.135	0.170	32	1251	24	5
B55.32	1.95	0.0055	0.135	0.170	32	1545	24	5
B75.32	1.95	0.0075	0.135	0.170	32	922	24	4
B85.24	1.95	0.0085	0.135	0.170	24	573	32	2
D15.48	2.10	0.0015	0.120	0.1385	48	1045	24	10
D30.48	2.10	0.0030	0.120	0.1385	48	469	24	3
D45.32sc	2.10	0.0045	0.0937	0.1077	32	1887	24	10

Table 1: The ensembles used in this investigation. For the labeling we employ the notation of ref. [10]. Additionally, we give the number of configurations N_{conf}, the number of stochastic samples N_s for all ensembles and the bootstrap block length N_b. The D30.48 ensemble was not yet included in Ref. [6].

will not investigate different matching observables for the charm quark and use only one μ_c-value. It is obtained by matching $aM_{K^+} = aM_K$ to determine $a\mu_s$. The latter is then used to obtain $a\mu_c$ via the relation Eq. (2.3).

For the extraction of quark masses and pseudo-scalar decay constants it turned out that using M_{K^+} for the matching lead to the smallest lattice artifacts [20]. However, this may depend on the quantities under consideration.

3. Pseudoscalar flavour-singlet mesons

In order to study properties of pseudoscalar flavour-singlet mesons we have to consider light strange and charm contributions to build a suitable correlation function matrix. Hence, in the physical basis we are after computing

$$\mathscr{C}(t) = \begin{pmatrix} \eta_\ell(t)\eta_\ell(0) & \eta_\ell(t)\eta_s(0) & \eta_\ell(t)\eta_c(0) \\ \eta_s(t)\eta_\ell(0) & \eta_s(t)\eta_s(0) & \eta_s(t)\eta_c(0) \\ \eta_c(t)\eta_\ell(0) & \eta_c(t)\eta_s(0) & \eta_c(t)\eta_c(0) \end{pmatrix}, \tag{3.1}$$

involving the following interpolating operators

$$\eta_\ell \equiv (\bar{\psi}_u i\gamma_5 \psi_u + \bar{\psi}_d i\gamma_5 \psi_d)/\sqrt{2}, \quad \eta_s \equiv (\bar{\psi}_s i\gamma_5 \psi_s), \quad \eta_c \equiv (\bar{\psi}_c i\gamma_5 \psi_c). \tag{3.2}$$

Since we are working in the twisted basis we have to rotate these operators. Let us start with the unitary action, where the rotation in the light sector is given by [5]

$$\frac{1}{\sqrt{2}}(\bar{\psi}_u i\gamma_5 \psi_u + \bar{\psi}_d i\gamma_5 \psi_d) \quad \rightarrow \quad \frac{1}{\sqrt{2}}(-\bar{\chi}_u \chi_u + \bar{\chi}_d \chi_d) \equiv \mathscr{O}_\ell, \tag{3.3}$$

where the left- and right-hand side correspond to physical and twisted basis, respectively. Also for strange and charm we have to consider a doublet as follows

$$\begin{pmatrix} \bar{\psi}_c \\ \bar{\psi}_s \end{pmatrix}^T i\gamma_5 \frac{1 \pm \tau^3}{2} \begin{pmatrix} \psi_c \\ \psi_s \end{pmatrix} \quad \rightarrow \quad \begin{pmatrix} \bar{\chi}_c \\ \bar{\chi}_s \end{pmatrix}^T \frac{-\tau^1 \pm i\gamma_5 \tau^3}{2} \begin{pmatrix} \chi_c \\ \chi_s \end{pmatrix} \equiv \mathscr{O}_{c,s}. \tag{3.4}$$

The flavour space projector $(1 \pm \tau^3)/2$ distinguishes between charm and strange contributions in the physical basis. In the twisted basis we need to consider the following operators when calculating correlation functions

$$\begin{aligned} \mathscr{O}_c &\equiv Z(\bar{\chi}_c i\gamma_5 \chi_c - \bar{\chi}_s i\gamma_5 \chi_s)/2 - (\bar{\chi}_s \chi_c + \bar{\chi}_c \chi_s)/2, \\ \mathscr{O}_s &\equiv Z(\bar{\chi}_s i\gamma_5 \chi_s - \bar{\chi}_c i\gamma_5 \chi_c)/2 - (\bar{\chi}_s \chi_c + \bar{\chi}_c \chi_s)/2. \end{aligned} \tag{3.5}$$

Note that the ratio of renormalisation constants Z appears in the sum of pseudoscalar and scalar currents. However, Z is not needed for extracting the masses of η and η', as we explain in Ref. [6]. For further details on how to construct the correlation matrix we also refer to Ref. [6].

Let us now discuss the rotation for the mixed action approach with OS valence strange and charm quarks. For the light quarks the operator is identical to the unitary one in Eq. (3.3), i.e. $\mathscr{O}_\ell^{\text{OS}} \equiv \mathscr{O}_\ell$. But for strange and charm quarks the operators are significantly simpler, due to no flavour mixing in between strange and charm:

$$\begin{aligned} \frac{1}{\sqrt{2}}(\bar{\psi}_c i\gamma_5 \psi_c + \bar{\psi}_{c'} i\gamma_5 \psi_{c'}) &\rightarrow \frac{1}{\sqrt{2}}(\bar{\chi}_c \chi_c - \bar{\chi}_{c'} \chi_{c'}) \equiv \mathscr{O}_c^{\text{OS}}, \\ \frac{1}{\sqrt{2}}(\bar{\psi}_s i\gamma_5 \psi_s + \bar{\psi}_{s'} i\gamma_5 \psi_{s'}) &\rightarrow \frac{1}{\sqrt{2}}(\bar{\chi}_s \chi_s - \bar{\chi}_{s'} \chi_{s'}) \equiv \mathscr{O}_s^{\text{OS}}. \end{aligned} \tag{3.6}$$

Again, we build a correlation function matrix of the form given in Eq. (3.1). Obviously, there is no mixing of pseudoscalar and scalar currents like in Eq. (3.5) and, therefore, no ratio of renormalisation constants appears.

For both, the unitary and the mixed action approach we solve the generalised eigenvalue problem [21, 22, 23]

$$\mathscr{C}(t)\, \eta^{(n)}(t,t_0) = \lambda^{(n)}(t,t_0)\, \mathscr{C}(t_0)\, \eta^{(n)}(t,t_0). \tag{3.7}$$

Taking into account the periodic boundary conditions for a meson and solving

$$\frac{\lambda^{(n)}(t,t_0)}{\lambda^{(n)}(t+1,t_0)} = \frac{e^{-m^{(n)}t} + e^{-m^{(n)}(T-t)}}{e^{-m^{(n)}(t+1)} + e^{-m^{(n)}(T-(t+1))}} \tag{3.8}$$

we determine the effective masses $m^{(n)}$, where n counts the eigenvalues. The state with the lowest mass should correspond to the η and the second state to the η' meson. Alternatively, we use a factorising fit of the form

$$\mathscr{C}_{qq'}(t) = \sum_n \frac{A_{q,n} A_{q',n}}{2m^{(n)}} \left[\exp(-m^{(n)}t) + \exp(-m^{(n)}(T-t)) \right] \tag{3.9}$$

to the correlation matrix matrix $\mathscr{C}$. The amplitudes $A_{q,n}$ correspond to $\langle 0|\bar{q}q|n\rangle$ with $n \equiv \eta, \eta', ...$ and $q = \ell, s, c$. Note that for this physical interpretation of the amplitudes the ratio of renormalisation constants Z is unavoidably required as input for the unitary approach [6].

3.1 Variance reduction

In general the correlation functions consist of quark connected and disconnected diagrams. The connected pieces have been calculated via the so called "one-end-trick" [24] using stochastic timeslice sources. For the disconnected diagrams we resort to stochastic volume sources with complex Gaussian noise. The light disconnected contributions can be estimated very efficiently using the identity [5]

$$D_u^{-1} - D_d^{-1} = -2i\mu_\ell D_d^{-1} \, \gamma_5 \, D_u^{-1} \, . \tag{3.10}$$

In the heavy sector of the unitary setup such a simple identity does not exist. Instead we use the (less efficient) so called hopping parameter variance reduction, which relies on the same identity as in the mass degenerate two flavour case (see ref. [24] and references therein). The number of stochastic volume sources N_s per gauge configuration we used for both the heavy and the light sector is given for each ensemble in table 1. In order to check that the stochastic noise introduced by our method is smaller than the gauge noise we have increased N_s from 24 to 64 for ensemble $B25.32$, which did not reduce the error on the extracted masses.

For OS strange and charm quarks the variance reduction trick Eq. (3.10) is also applicable, as noted in Ref. [9]. Consider the disconnected contributions for the operator in Eq. (3.6). Again, we may write for the strange quark

$$D_s^{-1} - D_{s'}^{-1} = -2i\mu_s D_{s'}^{-1} \, \gamma_5 \, D_s^{-1} \, , \tag{3.11}$$

and similarly for the charm quark. This identity can be used like in the light sector to compute the disconnected contributions of strange and charm quarks to the OS correlator matrix with greatly reduced noise [9].

4. Results from Unitary Strange and Charm Quarks

Most of the unitary results have already been published in Ref. [6], the only exception is ensemble $D30.48$. However this additional point does only very mildly affect the final results.

We have calculated all required contractions for the correlator matrix using local and fuzzed operators, yielding a 6×6-matrix. The number of gauge configurations per ensemble is given in Table 1. All errors have been calculated from bootstrapping with 1000 samples. To compensate for autocorrelation we have used blocking, the number of configuration per block N_b is also given in Table 1 and it was chosen such that the resulting blocklength in HMC trajectories N_{HMC} fulfils $N_{\text{HMC}} \geq 20$. For a more detailed discussion on autocorrelation, which mainly affects the η'-state we refer to [6].

4.1 Extraction of Masses

The details of our GEVP and fitting procedures to extract η and η' masses are explained in Ref. [6]. In Figure 1 we show the masses of the η (filled symbols) and η' (open symbols) mesons
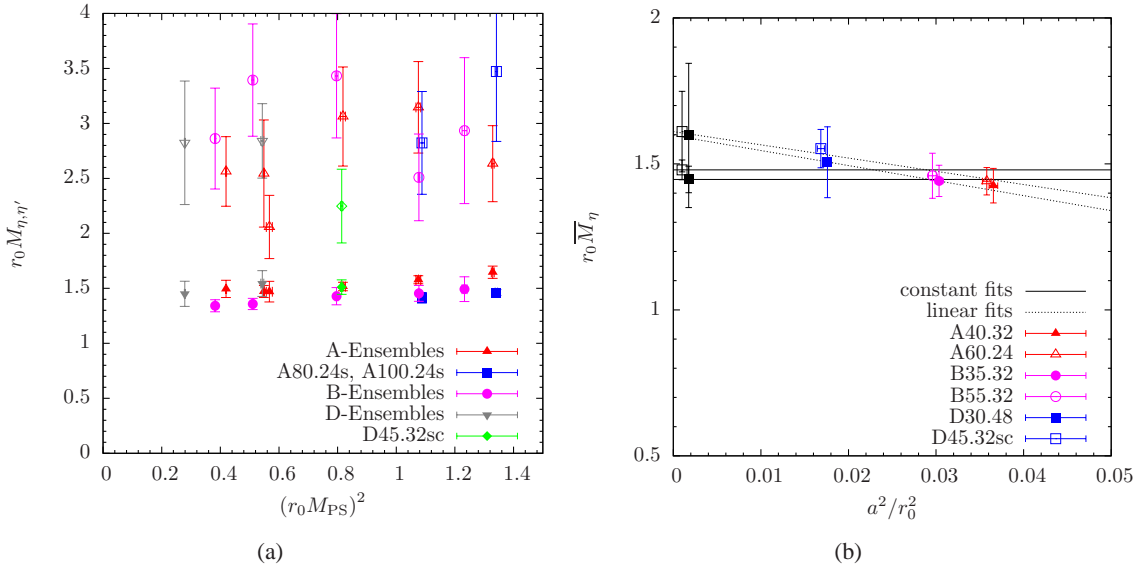
Figure 1: (a) η (filled symbols) and η' (open symbols) masses in units of r_0. (b) $r_0\overline{M}_\eta$ as a function of $(a/r_0)^2$ for the ensemble sets S_1 and S_2.

for the various ensembles we used as a function of the squared pion mass, everything in units of r_0. The values of the chirally extrapolated r_0^χ for each value of β can also be found in Ref. [6]. We present the values for aM_η and $aM_{\eta'}$ together with kaon and pion mass values in Table 2 with statistical errors only for the two ensembles $D30.48$ and $D45.32sc$. The results for $D30.48$ are new compared to what was shown in Ref. [6]. $D45.32sc$ will be used for the mixed action analysis. All other results can be found in Ref. [6].

It is clear from the figure that the η meson mass can be extracted with high precision, while the η' meson mass is more noisy.

4.2 Scaling Artifacts and Strange Quark Mass Dependence of M_η

The results displayed in the left panel of Figure 1 have been obtained using the bare values of $a\mu_\sigma$ and $a\mu_\delta$ as used for the production of the ensembles. Those values, however, did not lead to the physical values of, e.g., the kaon and D-meson masses [10, 19].

For M_η the statistical uncertainty is sufficiently small to attempt to correct for the mismatch in the strange quark mass value and to try a scaling test. For this we need to compare M_η at the three different values of the lattice spacing for fixed values of for instance r_0M_K, r_0M_D, r_0M_{PS} and the physical volume. From volume and the charm quark mass value we expect only little influence given our uncertainties and hence, we are going to disregard these minor effects in the following.

As discussed in Ref. [6], we have to perform an interpolation of M_η in M_K. For this purpose, we treat the masses of the η-meson and the kaon like in chiral perturbation theory as functions $M^2 = M^2[M_{PS}^2, M_K^2]$ and define the dimensionless derivative

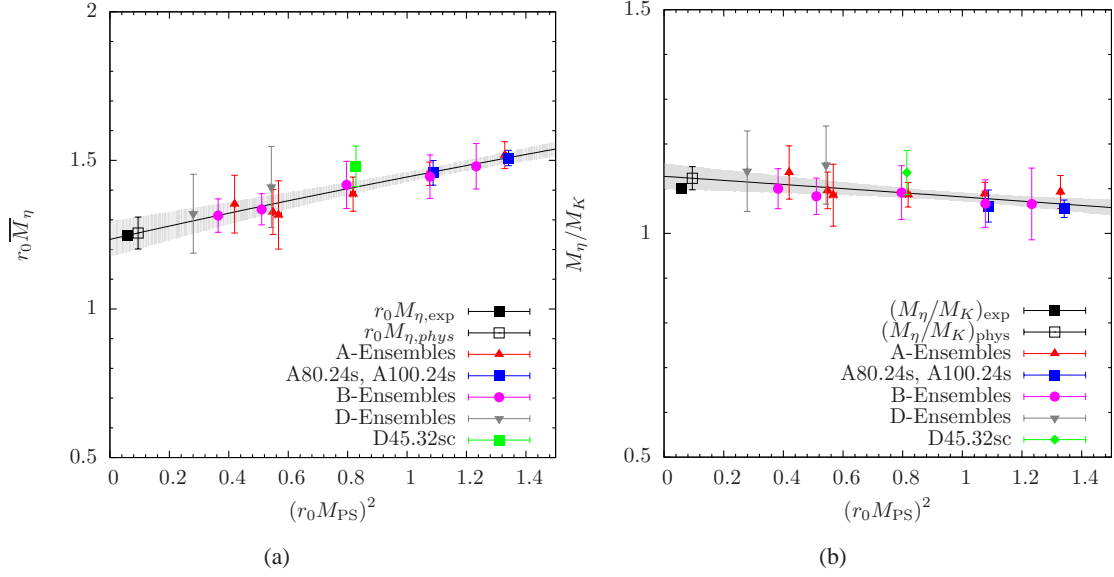$$D_\eta(\mu_\ell, \mu_\sigma, \mu_\delta, \beta) \equiv \left[\frac{d(aM_\eta)^2}{d(aM_K)^2}\right] . \tag{4.1}$$

7

Figure 2: (a) $r_0\overline{M}_\eta$ as a function of $(r_0M_{\rm PS})^2$. (b) $M_\eta/M_{\rm K}$ as a function of $(r_0M_{\rm PS})^2$.

Next we make the approximation that D_η is independent of the quark mass values $\mu_\ell, \mu_\sigma, \mu_\delta$ and β. Its value we can estimate from $A80.24$ and $A80.24s$ as well as from $A100.24$ and $A100.24s$. On average we obtain $D_\eta = 1.60(18)$.

Now we use this value of D_η to correct two sets S_1, S_2 of three ensembles, namely $S_1 = \{A40.32, B35.32, D30.48\}$ and $S_2 = \{A60.24, B55.24, D45.24\}$ to a common value of $r_0M_{\rm K} \approx 1.34$ using

$$(r_0\overline{M}_\eta)^2 = (r_0M_\eta)^2 + D_\eta \cdot \Delta_{\rm K},$$

where $\Delta_{\rm K}$ is the difference in the squared kaon mass values to the squared reference values (in units of r_0). For each set the three points have approximately fixed values of $r_0M_{\rm PS}$.

We plot the resulting $r_0\overline{M}_\eta$ values for sets $S_{1,2}$ as a function of $(a/r_0)^2$ in the right panel of Figure 1. Both data sets are still compatible with a constant continuum extrapolation giving $r_0M_{\eta,S_1,{\rm const}}^{\to 0} = 1.447(45)$ and $r_0M_{\eta,S_2,{\rm const}}^{\to 0} = 1.480(34)$, respectively, which we indicate by the horizontal lines. We can also perform a linear extrapolation, leading to $r_0M_{\eta,S_1,{\rm lin}}^{a\to 0} = 1.60(25)$ and $r_0M_{\eta,S_2,{\rm lin}}^{a\to 0} = 1.61(14)$, which is also shown in the figure. The difference in between the two extrapolated values for each set are

$$r_0\Delta M_{\eta,S_1}^{a\to 0} = 0.15(25), \quad r_0\Delta M_{\eta,S_2}^{a\to 0} = 0.13(13) \tag{4.2}$$

and they give us an estimate on the systematic uncertainty to be expected from the continuum extrapolation. Both results agree well, although the one for S_1 exhibits twice the error. We will therefore quote an 8% relative error from $\Delta M_{\eta,S_2}^{a\to 0}/M_{\eta,S_2,{\rm const}}^{a\to 0}$ for our mass estimates, which was already used in Ref. [6] where S_1 was not yet available.

In order to obtain a more complete picture, we now correct all our ensembles for the slightly mistuned value of $M_{\rm K}$. For this we follow the procedure which was discussed in detail in [6], i.e. we shift the kaon mass values for all ensembles to a common line $(r_0M_K)^2[(r_0M_{\rm PS})^2]$ determined such that it reproduces the physical kaon mass value at the physical point. Next we correct the η

ensemble	aM_{PS}	aM_{K}	aM_η	$aM_{\eta'}$
$D30.48$	0.09776(45)	0.17760(23)	0.205(16)	0.38(4)
$D45.32sc$	0.07981(30)	0.17570(84)	0.192(15)	0.30(4)

Table 2: Results of aM_η, $aM_{\eta'}$ for ensembles $D30.48$ and $D45.32sc$. and the corresponding values for the charged pion mass M_{PS} and the kaon mass M_{K}. The $D30.48$ is new compared to Ref. [6] and ensemble $D45.32sc$ is needed for the mixed action results. Results for all the other ensembles can be found in Ref. [6].

masses appropriately. The result of this procedure is shown in the left panel of Figure 2: we show values of the corrected η masses $r_0\overline{M}_\eta$ for all our ensembles as a function of $(r_0M_{\text{PS}})^2$. It is evident that all the data fall on a single curve within statistical uncertainties, which confirms that M_η is not affected by large cut-off effects. Note, however, that we again ignored possible μ_ℓ, μ_σ, μ_δ and β dependence with this procedure.

4.3 Extrapolation to the Physical Point

Since we have now fixed the strange quark mass to its physical value using $M_{\text{K}^0}^{\text{exp}} = 498$ MeV, we can attempt a linear fit to all corrected data points for $(r_0\overline{M}_\eta)^2[(r_0M_{\text{PS}})^2]$. Using $r_0 = 0.45(2)$ fm as in Ref. [11], the fit yields $r_0M_\eta \left[r_0^2M_\pi^2 \right] = 1.256(54)_{\text{stat}}(100)_{\text{sys}}$ and in physical units

$$M_\eta(M_\pi) = 551(33)_{\text{stat}}(44)_{\text{sys}} \text{ MeV} , \tag{4.3}$$

where the experimental mass-value of the neutral pion $M_{\pi^0} = 135$ MeV has been used for M_π. In the $SU(2)$ chiral limit we obtain $r_0M_\eta^0 = 1.230(65)_{\text{stat}}(98)_{\text{sys}}$ or $M_\eta^0 = 539(35)_{\text{stat}}(43)_{\text{sys}}$ MeV .

As the procedure used to correct the η mass for mistuning of the strange quark mass ignores a possible dependence on μ_ℓ, μ_σ, μ_δ and β, it is desirable to have a cross-check. In Ref. [6] we discussed two possible options for this. The first one is to study the ratio M_η/M_K, for which it was shown that most of the strange quark dependence cancels. The second possibility is to study the Gell-Mann-Okubo (GMO) relation which is motivated by chiral perturbation theory. Here we simply repeat the analysis for both cases, including the new data point for $D30.48$.

For the ratio $(M_\eta/M_K)^2$ a linear extrapolation for all available data in $(r_0M_{\text{PS}})^2$ to the physical pion mass point yields (see the shaded band in the right panel of Figure 2) $(M_\eta/M_{\text{K}})_{M_\pi} = 1.123(26)$, which agrees well with the experimental value $(M_\eta/M_{\text{K}})_{\text{exp}} = 1.100$. Using the experimental value of M_{K^0} we obtain $M_\eta = 559(13)_{\text{stat}}(45)_{\text{sys}}$ MeV. Note that in this analysis the scale $r_0 = 0.45(2)$ fm is only required for determining the physical pion mass point. As the slope of the extrapolation is rather small, the statistical uncertainty in M_η is significantly smaller than for the direct extrapolation of $(r_0M_\eta)^2$.

Considering the GMO relation and again performing a linear extrapolation in $(r_0M_{\text{PS}})^2$ including all available data we obtain $\left(3M_\eta^2/(4M_{\text{K}}^2 - M_\pi^2)\right)_{M_\pi} = 0.970(47)$ at the physical pion mass, which is in agreement with experiment, $(3M_\eta^2/(4M_{\text{K}}^2 - M_\pi^2))^{\text{exp}} = 0.925$. Using the experimental values of M_{π^0} and M_{K^0} we now obtain $M_\eta = 561(14)_{\text{stat}}(45)_{\text{sys}}$ MeV, where the first error is statistical and the second systematic estimated again from the scaling violations discussed above.
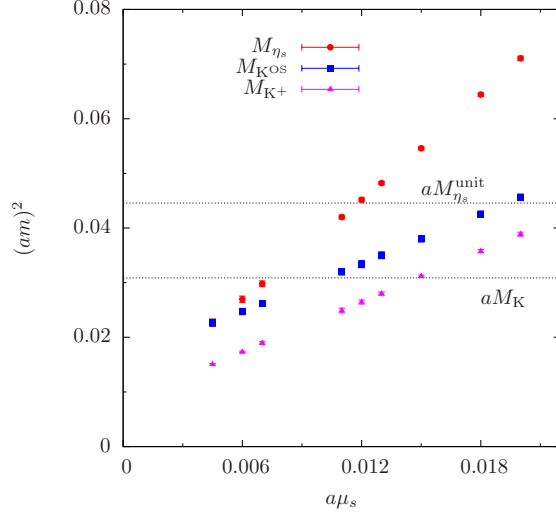
Figure 3: We show $(M_{\eta_s})^2$, $(M_{K^{OS}})^2$ and $(M_{K^+})^2$ extracted with OS-type valence quarks as functions of the bare OS strange quark mass $a\mu_s$. As horizontal lines we show the unitary values of $(aM_K)^2$ and $(aM_{\eta_s}^{\text{unit}})^2$.

5. Results using OS strange and charm quarks

In this section we will discuss first results for η and η' meson masses using OS strange and charm quarks. We focus here on one ensemble, namely *D45.32sc*, see Table 1.

For given values of $a\mu_\ell, a\mu_s$ and $a\mu_c$ we determine the correlation matrix Eq. (3.1) using the interpolating operators Eq. (3.3) and Eq. (3.6) using 900 configurations. Two consecutive configurations are spaced by 4 trajectories of length 1. Disconnected contributions are estimated using 32 Gaussian volume sources per gauge configuration. We use local and fuzzed operators and build correspondingly a 3×3 or 6×6 correlation function matrix. Errors are estimated using 1000 bootstrap samples. The data is blocked in blocks of length 5 to account for autocorrelations. Mass values of η and η' are extracted using the same methods as in the unitary case.

5.1 Matching The Strange Quark Mass

As discussed in Section 2, sea- and valence-actions can be matched using various different observables. We will consider here $M_{K^{OS}}$, M_{K^+} and M_{η_s}. In Figure 3 we show $(aM_{K^{OS}})^2$, $(aM_{K^+})^2$ and $(aM_{\eta_s})^2$ as functions of $a\mu_s$ for ensemble *D45.32sc*. We also show both $(aM_{\eta_s}^{\text{unit}})^2$ and $(aM_K)^2$ as horizontal lines. The value of aM_K can be found in Table 2. The value for $aM_{\eta_s}^{\text{unit}}$ has been determined using the connected contributions to the unitary correlator matrix only, and its value is $aM_{\eta_s}^{\text{unit}} = 0.2105(14)$.

From Figure 3 it is first of all clear that using different valence quantities leads to very different matching values for $a\mu_s$. Using for instance M_{K^+} leads to $a\mu_s = 0.0149(3)$, while matching $M_{K^{OS}}$ leads to $a\mu_s = 0.0102(3)$. Therefore, for this proceeding we decided to use the following three values for the bare OS strange quark mass

$$a\mu_s = 0.01,\ 0.0125,\ 0.018,\ 0.025.$$

These four values bracket the three matching values stemming from the different matching quantities. It is worth noting that the leftmost data points in Figure 3 correspond to the case where
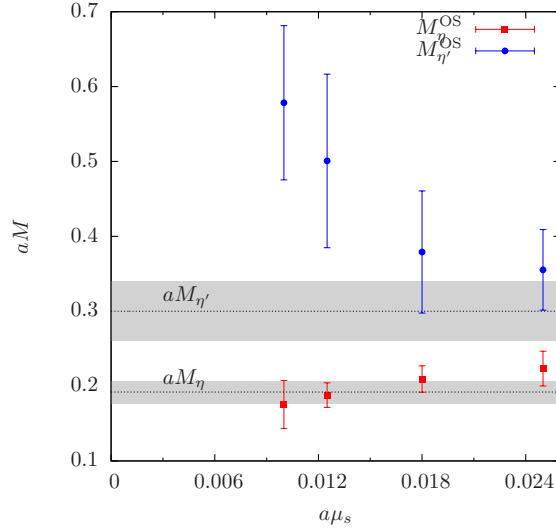
10

Figure 4: M_η^{OS} and $M_{\eta'}^{\mathrm{OS}}$ as a function of $a\mu_s$ for *D*45.32*sc*. In addition we show as horizontal lines the corresponding unitary masses with errors as shaded band. Note that for M_η and $M_{\eta'}$ we used higher statistics.

$a\mu_s = a\mu_\ell$. Hence, $aM_{\mathrm{K^{OS}}} = aM_{\eta_s}$. The splitting in between $aM_{\mathrm{K^{OS}}}$ and $aM_{\mathrm{K^+}}$ is an $\mathscr{O}(a^2)$ effect, which disappears in the continuum limit.

As mentioned before we do not expect the precise charm quark mass value to be important for η and η', which is also confirmed by our unitary results. Therefore, we use only one value $a\mu_c = 0.172$ for the OS bare charm quark mass. It is obtained by matching $aM_{\mathrm{K^+}} = aM_{\mathrm{K}}$ to determine $a\mu_s$. $a\mu_c$ is then obtained via the relation Eq. (2.3).

5.2 The valence strange quark mass dependence of the OS η states

In Figure 4 we show the lowest two states extracted from a 6×6 matrix as a function of the OS strange quark mass $a\mu_s$ for the *D*45.32*sc* ensemble. The state with the lowest mass should correspond to the η, the second to the η' state. In addition to the OS results we show as horizontal lines the unitary mass values discussed in the previous section (see Table 2). Note that the unitary values were produced with roughly twice the number of configurations but only 24 instead of 32 stochastic samples (cf. Table 1).

In general one observes from Figure 4 that the η mass value can be extracted with high statistical accuracy, while the η' suffers from similar noise as observed for the unitary η'. In fact, for the η meson mass we obtain slightly better accuracy as compared to the unitary case. However, the noise reduction trick applicable for OS strange and charm quarks does not seem to help for the extraction of the OS η' meson mass: in the effective mass plots a plateau is only hardly visible. Hence, we expect that the OS η' is affected by similarly large systematic uncertainties as the unitary η'.

Therefore, we consider in the following only the OS η meson and its μ_s dependence. It is interesting to understand which of the matching observables discussed above yields the best agreement in between OS and unitary η mass values. First of all, we observe a rather mild dependence of M_η^{OS} on the bare OS strange quark mass $a\mu_s$, see Figure 4. In order to compare to the unitary
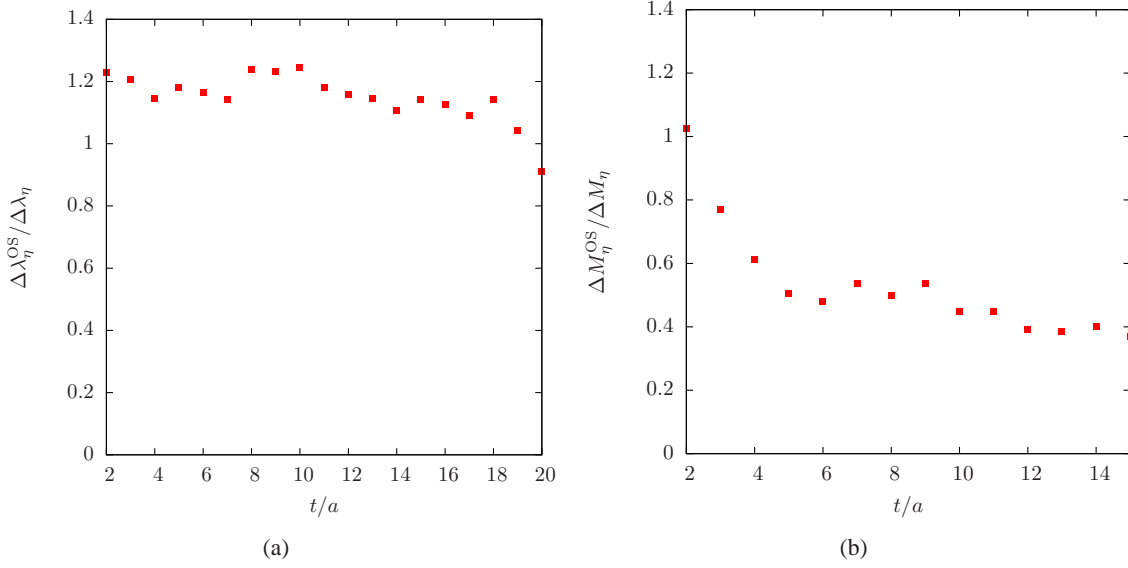
Figure 5: (a) We show the OS to unitary ratio of relative errors of the η-eigenvalue as a function of t/a. (b) the same as (a) but for the effective masses.

case, we compute

$$D_\eta^{\mathrm{OS}} \equiv \left[\frac{d(M_\eta^{\mathrm{OS}})^2}{d(M_{\mathrm{K}^+})^2} \right] = 0.8(1)$$

with statistical error only, and compare to $D_\eta = 1.60(18)$ defined in Eq. 4.1. The OS value is significantly smaller which we attribute to the large sea quark contributions to the η meson mass.

As a consequence, the OS η mass agrees within errors with the unitary η mass value for all $a\mu_s$ values considered. The agreement is best around the M_{K^+} matching point, though. Given the large uncertainties in the OS η' meson mass, we find also for the η' meson masses at least marginal agreement within errors. However, one should keep in mind the potentially large systematics affecting the η' mass determination.

5.3 Comparing OS and Unitary Approach

It is also interesting to compare OS and unitary approach on a correlator level. For this we computed the correlator matrix Eq. (3.1) for $D45.32sc$ on the same set of configurations with identical number of stochastic samples, namely $N_s = 24$. For both cases the GEVP is solved and the eigenvalues with errors are extracted. We then compare in the left panel of Figure 5 the relative errors of the eigenvalues corresponding to the η state λ_η by plotting the ratio $\Delta\lambda_\eta^{\mathrm{OS}}/\Delta\lambda_\eta$ as a function of t/a. This ratio is slightly larger or close to 1. However, the same ratio for the effective masses shown in the right panel of Figure 5 is from $t/a = 5$ on equal or smaller than $1/2$.

This apparent contradiction is explained by a correlation between $\lambda_\eta^{\mathrm{OS}}(t/a)$ and $\lambda_\eta^{\mathrm{OS}}(t/a+1)$ very close to one for all t/a in the OS case. For the unitary case the same correlation coefficient is smaller or equal to 0.8. For this reason the η meson mass can be determined with slightly better accuracy from the OS analysis than from the unitary one. The reason is likely to be the variance reduction trick for OS strange quarks, as the η has a larger strange than light contribution.

6. Summary and Outlook

In this proceeding contribution we presented an update of our investigation of η and η' meson properties using $N_f = 2+1+1$ flavour of Wilson twisted mass fermions, first published in Ref. [6]. We added one additional ensemble at the finest available lattice spacing. This allows us to estimate systematics from the continuum extrapolation with higher confidence. The final result for the η meson mass at the physical point stays virtually unchanged compared to Ref. [6]

$$M_\eta = 558(14)_{\text{stat}}(45)_{\text{sys}} \text{ MeV}.$$

In addition we presented an exploratory investigation with a mixed action, where valence strange and charm quarks are regularised as so called Osterwalder-Seiler fermions. For one ensemble $D45.32sc$ we matched valence and unitary actions using M_η. The obtained OS bare strange quark mass is in good agreement to the one obtained using kaons for matching.

It turns out that in the OS approach the η can be determined with slightly higher statistical accuracy compared to the unitary case, when the number of inversions is approximately matched. However, the η' is still noisy and we cannot determine it with higher accuracy than in the unitary case. The OS η mass shows a smaller dependency on the OS kaon mass than the unitary η mass on the unitary kaon mass, which we attribute to significant sea quark contributions to the η meson.

In a next step we plan to improve the η' meson mass determination. This could be reached by using the point-to-point method described in Ref. [5] and/or by increasing our operator basis. Moreover, we will study the continuum extrapolation of the OS η meson mass for different matching conditions.

Acknowledgements

References

[1] N. Christ *et al.*, Phys.Rev.Lett. **105**, 241601 (2010), `arXiv:1002.2999`.

[2] **TWQCD/JLQCD** Collaboration, T. Kaneko *et al.*, PoS **LAT2009**, 107 (2009), `arXiv:0910.4648`.

[3] J. J. Dudek *et al.*, Phys.Rev. **D83**, 111502 (2011), `arXiv:1102.4299`.

[4] E. B. Gregory, A. C. Irving, C. M. Richards and C. McNeile, `arXiv:1112.4384`.

[5] **ETM** Collaboration, K. Jansen, C. Michael and C. Urbach, Eur.Phys.J. **C58**, 261 (2008), arXiv:0804.3871.

[6] **ETM collaboration** Collaboration, K. Ottnad, C. Michael, S. Reker and C. Urbach, arXiv:1206.6719.

[7] **ALPHA** Collaboration, R. Frezzotti, P. A. Grassi, S. Sint and P. Weisz, JHEP **08**, 058 (2001), hep-lat/0101001.

[8] R. Frezzotti and G. C. Rossi, JHEP **10**, 070 (2004), arXiv:hep-lat/0407002.

[9] **ETM Collaboration** Collaboration, S. Dinter *et al.*, JHEP **1208**, 037 (2012), arXiv:1202.1480.

[10] **ETM** Collaboration, R. Baron *et al.*, JHEP **06**, 111 (2010), arXiv:1004.5284.

[11] R. Baron *et al.*, PoS **LATTICE2010**, 123 (2010), arXiv:1101.0518.

[12] R. Frezzotti and G. C. Rossi, Nucl. Phys. Proc. Suppl. **128**, 193 (2004), hep-lat/0311008.

[13] T. Chiarappa *et al.*, Eur. Phys. J. **C50**, 373 (2007), arXiv:hep-lat/0606011.

[14] R. Frezzotti and G. C. Rossi, JHEP **08**, 007 (2004), hep-lat/0306014.

[15] **ETM** Collaboration, C. Urbach, PoS **LAT2007**, 022 (2007), arXiv:0710.1517.

[16] P. Dimopoulos, R. Frezzotti, C. Michael, G. Rossi and C. Urbach, Phys.Rev. **D81**, 034509 (2010), arXiv:0908.0451.

[17] **ETM** Collaboration, R. Baron *et al.*, JHEP **1008**, 097 (2010), arXiv:0911.5061.

[18] **ETM** Collaboration, B. Blossier *et al.*, JHEP **04**, 020 (2008), arXiv:0709.4574.

[19] **ETM** Collaboration, R. Baron *et al.*, Comput.Phys.Commun. **182**, 299 (2011), arXiv:1005.2042.

[20] S. R. Sharpe and J. M. Wu, Phys.Rev. **D71**, 074501 (2005), arXiv:hep-lat/0411021.

[21] C. Michael and I. Teasdale, Nucl.Phys. **B215**, 433 (1983).

[22] M. Lüscher and U. Wolff, Nucl.Phys. **B339**, 222 (1990).

[23] B. Blossier, M. Della Morte, G. von Hippel, T. Mendes and R. Sommer, JHEP **0904**, 094 (2009), arXiv:0902.1265.

[24] **ETM** Collaboration, P. Boucaud *et al.*, Comput.Phys.Commun. **179**, 695 (2008), arXiv:0803.0224.

[25] K. Jansen and C. Urbach, Comput.Phys.Commun. **180**, 2717 (2009), arXiv:0905.3331.

[26] **ETM** Collaboration, A. Deuzeman, S. Reker and C. Urbach, arXiv:1106.4177.

[27] R Development Core Team, *R: A language and environment for statistical computing*, R Foundation for Statistical Computing, Vienna, Austria, 2005, ISBN 3-900051-07-0.